Available on CMS information server

CMS NOTE 1998/051

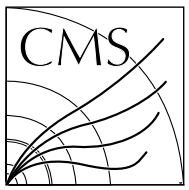

The Compact Muon Solenoid Experiment

CMS Note

Mailing address: CMS CERN, CH-1211 GENEVA 23, Switzerland

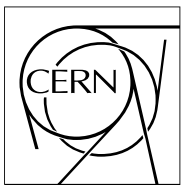

July 28, 1998

Simulation of the DTBx Drift Cell with an Improved Software Package

T. Rovelli

INFN e Dipartimento di Fisica, Università di Bologna, Bologna, Italy

Abstract

A new package was used to study the performance of the CMS barrel muon drift cell with a different configuration of the cathodes and cell dimensions.

Introduction

In a previous note[1], a procedure to include the dielectric materials in the simulation of the drift cell was described. The method relays on the Poisson package[2], to calculate the potential and the electrostatic field in the drift cell using a correct parameterization of the dielectric materials. These data are then given as input to the GARFIELD package[3] which has a very powerful description of the drift and amplification processes in wire chambers.

The Poisson package has two major shortcomings:

- the minimum step size is too coarse to describe the wire
- changes in the geometry of the cell are very laborious to implement.

In this note we present the results obtained using a new package, MAXWELL[4], instead of POISSON, for the simulations of several versions of the CMS muon barrel drift cell.

Comparison of a drift cell simulation using MAXWELL and POISSON

MAXWELL is a user friendly interactive programs which allows to define the cell structure and implement changes in a very straightforward and efficient way. In this respect it is much more powerful than POISSON. MAXWELL also allows to define very small step sizes and it can therefore describe the wire dimensions correctly.

To check the performance of the two packages we have simulated with MAXWELL the TDR baseline drift cell (MB96) and we have compared the results with those obtained with POISSON.

The MB96 cell parameters are:

- Cell width = 4.0 cm; height = 11. mm
- Strip width = 14. mm on 20mm wide mylar
- Lexan Isolated I-beams
- $50.\mu$m diameter stainless steel wire

The behaviour of the cell was simulated assuming standard operating conditions:

- Ar CO_2 $(85:15)$ gas mixture
- -1800 V (cathode); 1800 V (strip); 3600 V(wire).

As a monitor of the cell performance we have chosen the drift time of electrons generated along a line normal to the ground planes (y-axis) at four different distances from the cathode:

x = 0.1cm; x = 0.7 cm; x = 1.2 cm and x = 1.7 cm.

Differences up to 3.% are visible in the distributions of the drift times shown in Figure 1. The simulation done with MAXWELL gives systematically shorter drift times for electrons generated in the region near the ground planes with the largest differences in proximity of the cathode.

In the region near the midplane of the cell, which is most important for the charge collection, the results of the two simulations are in excellent agreement.

Part of the observed differences can be ascribed to the parameterization of the cathode which is done independently in the two programs. For the purpose of this work it is therefore safe to assume that the two packages give consistent results.

In the following we will present results based only on MAXWELL and GARFIELD.

Performance of the drift Cell with new I-beams

In the baseline MB96 drift cell, see Figure 2, the cathodes are made of lexan insulated aluminum I-beams. In this design the lexan strips are glued to the bases of the I-beams which are later glued to the aluminum ground planes.

Mechanical tests have shown that this structure does not have adequate rigidity expecially for the larger chambers.

An alternative design where the cathodes are made by attaching a mylar insulated electrode to the I-beams, see Figure 2, has become an interesting option. The electrode is formed by attaching a 100.μm thick 17mm wide mylar tape to an aluminum I-beam with 14 mm wide bases and then attaching a 35.μm thick 11. mm wide copper tape on the mylar. The copper is centered on the mylar thus leaving 3.mm of insulation at each side. At the extremities of the I-beam the copper is cut 5.mm inside the I-beam. This structure of the cathodes results in a mechanically stronger chamber since the mechanical function of the I-beams is decoupled from the electrical one and the I-beams can be glued directly to the ground planes.

To assess the impact of changing the cathode structure on the cell performances, we have simulated the MB96 cell and another cell (C98B) which differed only in the cathode design.

The equipotential lines calculated by MAXWELL are given in Figure 3 for the two drift cells. For mechanical and electrical reasons the electrode on the new cathode cannot reach the ground plane thus, near the cathode, the effective cell is reduced with respect to MB96. Furthermore the electric field is much stronger near the cathode than in MB96. This is shown in Figure 4. where the electric field is given at the center of the cell for the two drift cells.

To investigate further the performances of the cells we give in Figure 5 to 8 the drift lines for electrons generated at four distances from distances from the cathode:

x = 0.1cm; x = 0.7 cm; x = 1.2 cm and x = 1.7 cm.

As expected the major differences occur in the drift lines of electrons generated near the cathode. In this region the strong field generated by the new cathodes drifts the electrons toward the ground plane thus reducing significantly the charge collection efficiency. The drift time of the electrons generated at the 4 x positions are given in Figure 9 for the two drift cells. Taking as a figure of merit the δy interval of the cell were the collected charge reaches the wire within 20 ns, one can conclude that at x=0.1 cm from the cathode only 2-3 mm around the midplane are efficient with the new cathodes. However in the other positions the performance of the new cell is better of equal to those of MB96.

Optimization of the drift Cell with new I-beams

Once the dimensions of the cell and the structure of the cathodes are fixed, the only parameter left to optimize the field configuration is the strip width. The cell performance can be adjusted further by changing the operating voltages of the cathodes, strips and the anode wire.

This is a multidimensional space which is quite time consuming to explore.

As a first attempt to optimize the drift cell we have chosen the following operating voltages:
-1600 V (cathode); 1900 V (strip); 3600 V(wire) and the following strip widths:
12mm, 14mm, 16mm, 17mm and 18mm.

Furthermore the cell width was increased to 4.2 cm. This is the proposed new baseline value that optimizes the readout granularity and also gives a substantial cost reduction.

The drift field as a function of the wire distance is given in Figure 10 for the various strip widths. The best performance is obtained with a 17mm wide strip which produces the most uniform drift field.

Since the field near the cathode is very high, the uniformity of the drift field can be improved by keeping a low voltage (absolute value) on the cathode and increasing the voltage on the wire.

Before attempting the optimization of the HV operating values we have changed the distance between the ground planes from 11. mm to 11.5 mm to match the proposed baseline chamber design which uses 1.5 mm thick aluminum plates instead of 2.0 mm used in the TDR design.

With this *final* drift cell configuration we have studied several possible operating voltages, see table 1, grouped by:
$V_{amp} \simeq V_{wire} - V_{strip}$, and :
$V_{drift} \simeq V_{wire} - V_{cathode}$.

All these operating conditions give acceptable drift field quality. As an example, see Figure 11, the field uniformity for the *final* cell operating at :
-1400 V (cathode); 1800 V (strip); 3700 V(wire) is as good as for MB96 at the standard operating voltages:
-1800 V (cathode); 1800 V (strip); 3600 V(wire).

With these voltages the drift field in the *final* cell is considerably lower than for MB96 but it is still amply sufficient to ensure a saturated drift velocity as is shown in Figure 12, where the drift velocity calculated by GARFIELD is given as a function of the drift field at 300^{o} K and typical ambient pressure 730 and 770 mbar.

Table 1: High Voltage Operating values considered.

High Voltage (V)	V_{drift}	V_{AMP}
-1500;1800;3600	5100	1800
-1400;1900;3700	5100	1800
-1500;1900;3700	5200	1800
-1500;2000;3800	5300	1800
-1400;1800;3700	5100	1900
-1400;1900;3800	5200	1900
-1500;1900;3800	5300	1900
-1500;2000;3900	5400	1900
-1600;1900;3800	5400	1900
-1300;1800;3800	5100	2000

Additional studies of the drift Cell with new I-beams

The sharp edge of the electrode on the new I-beam is a source of concern since electrons might be extracted by the strong field thus increasing the cathode dark current or might drift to the anode wire creating an excessive high current in the chamber. To study this effect we have generated electrons along a line in proximity of the edge of the cathode electrode and also in proximity of the strip edge.

The drift lines of these electrodes for the cell operating at:
-1600 V (cathode); 1900 V (strip); 3600 V(wire)
are shown in Figure 13. It is quite evident that all the electrons that might be extracted from the cathode's edge are drifted toward the ground plates. No drift line connect the edge of the cathode to the anode wire. This of course is true only in two dimensions, i.e. along the cathode. At the extremities of the I-beams electrons extracted near the center of the cathode edge can be drifted toward the wire. It is therefore necessary to isolate these spots during the chamber construction.

For the strip above the wire the situation is quite different since it is charged to a positive potential hence the electrons cannot be extracted but instead electrons generated in its proximity will drift unto the strip.

Another concern is the possibility that positive ions might drift unto the mylar and create an electrostatic charge that might deform the field locally. This effect has been studied by generating positive ions in proximity of the anode wire and drifting them out in the cell. The drift lines are shown in Figure 14 for ions generated along the y axis and the x axis. In either case the drift lines end up in narrow regions respectively at the cathode and the strip.

Summary and conclusions

There is a good agreement between the descriptions of the drift cell electrical properties obtained with MAXWELL and Poisson.

However it is much easier and faster to change the drift cell parameters in MAXWELL than in Poisson. This has made possible to study a large variety of drift cell conditions in a short time.

We have studied the performance of the DTBx drift cell with a new design of the cathode which strengthens the mechanical structure of the chamber while retaining the main features of the baseline design.

The dimension of the strip electrode was optimized for the *final* cell dimensions with the new cathodes.

The optimized *final* final drift cell was found to give good performance over a wide range of operating voltages and to reach the same level of drift field uniformity as the MB96 cell albeit with a reduced charge collection efficiency in proximity of the cathode.

Acknowledgements

I would like to thank A.Benvenuti for the stimulating discussion and for the help given to me during the entire development of this work.

I would like to thank as well R.Veenhof, for his help in using some of the new Garfield features and for his availability in testing the actual cell configuration.

References

[1] **CMS TN/95 - 106**, T. Rovelli, *" Simulation of the CMS Barrel Muon Chambers "*.

[2] C. Iselin, *" Solution of Poisson's or Laplace's Equation in Two-Dimensional Region "* CERN Program Library T604 1982.

[3] R. Veenhof, *" Garfield, a Drift-Chamber Simulation Program User's Guide "* CERN Program Library W5050 1994.

[4] ANSOFT, *" Maxwell 2D Parameter Extractor User's Reference "* ANSOFT Corporation

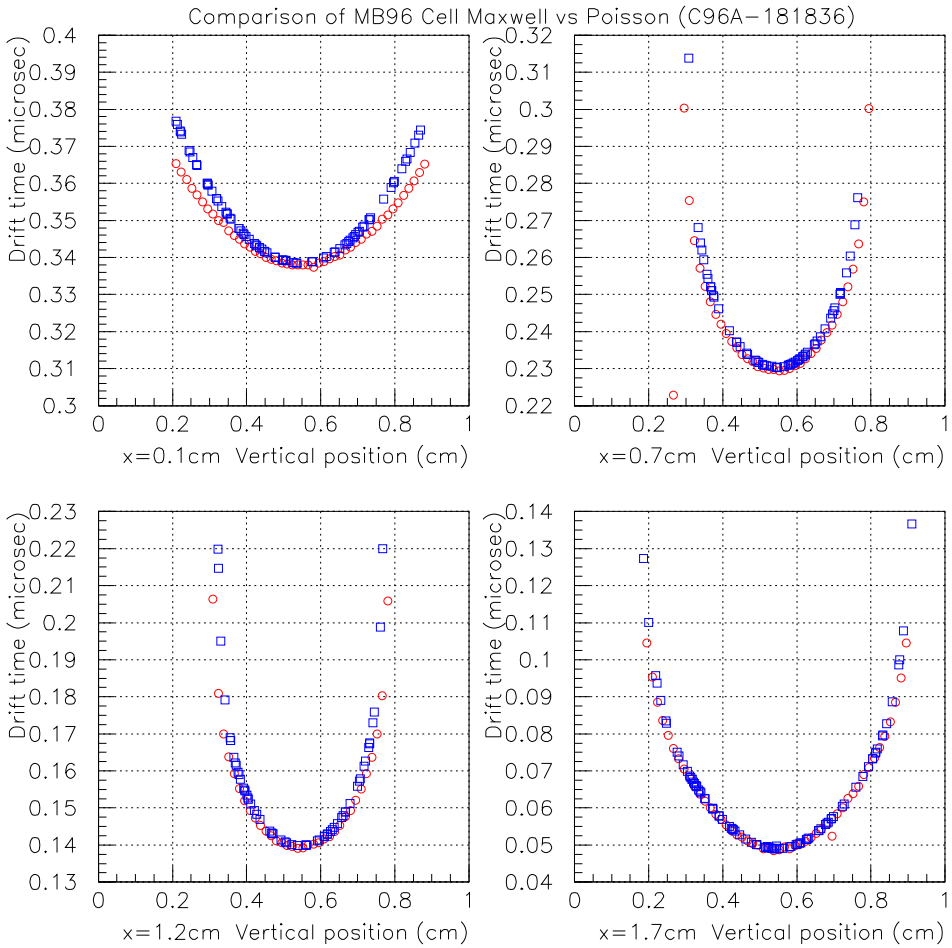

Figure 1: Comparison of drift time at different distances from the cathode as calculated by MAXWELL (open circles) and POISSON (squares)

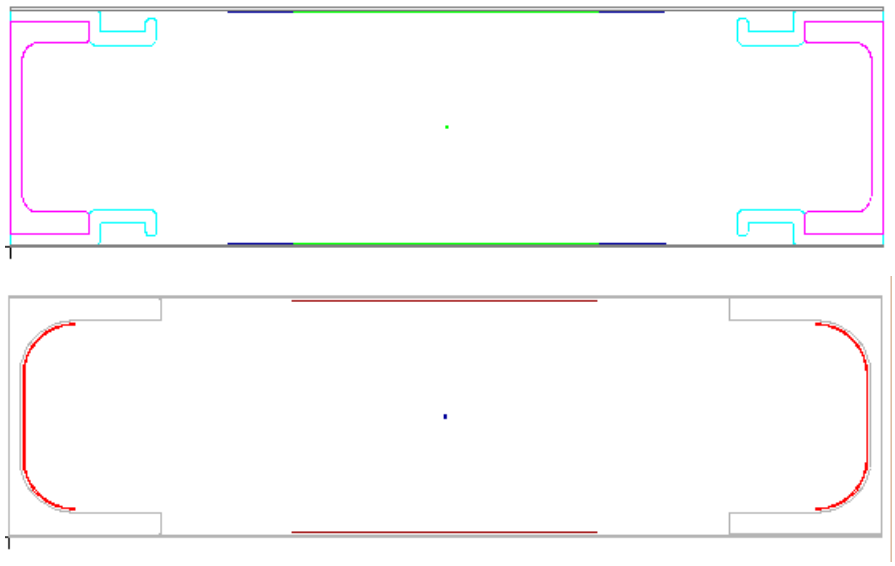

Figure 2: MB96 drift cell representation in MAXWELL: with lexan isolated I-beams (top) and with the new cathodes (bottom)

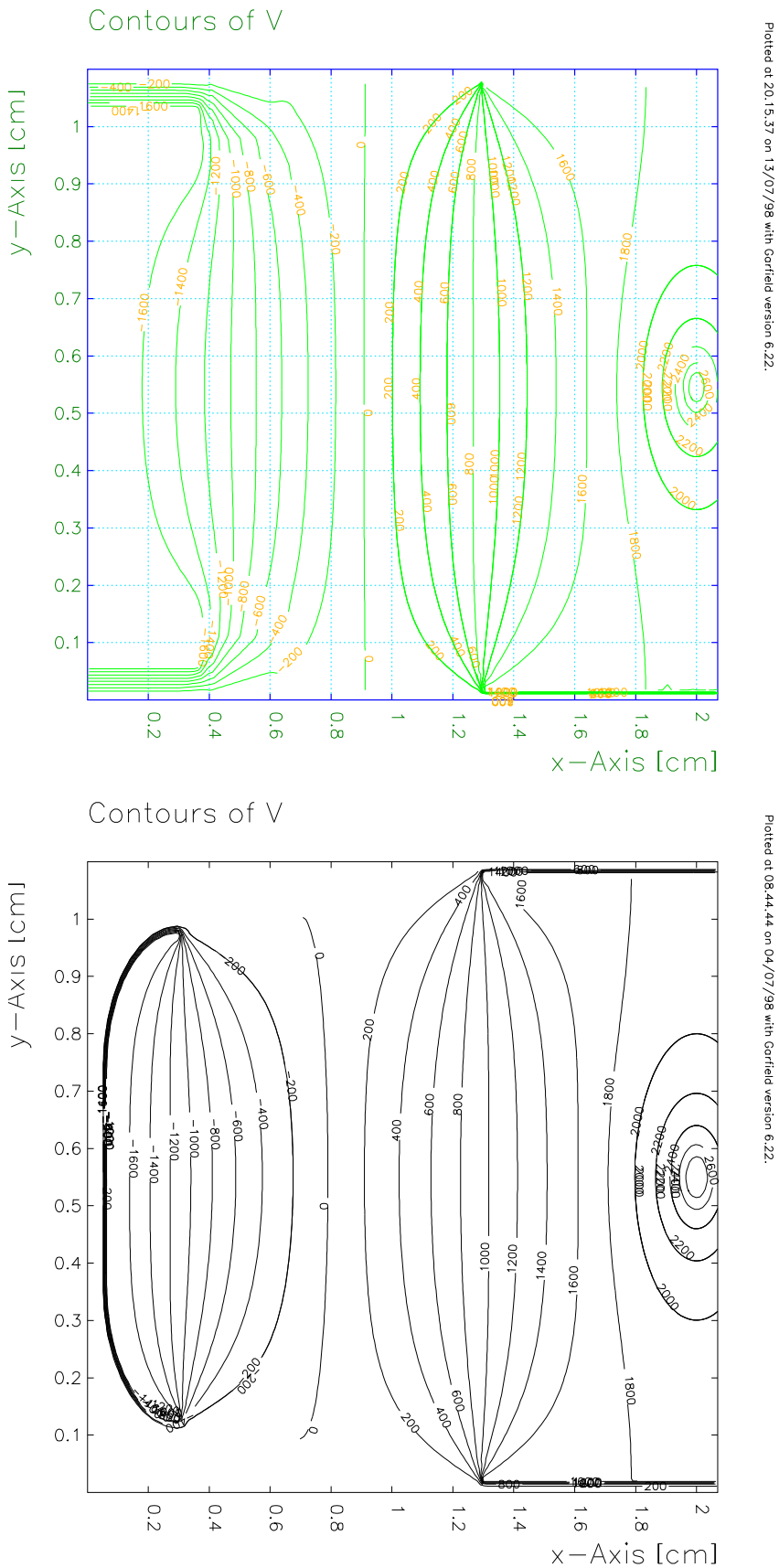

Figure 3: Equipotential lines for MB96 drift cell (top) and for the cell with new cathodes (bottom)

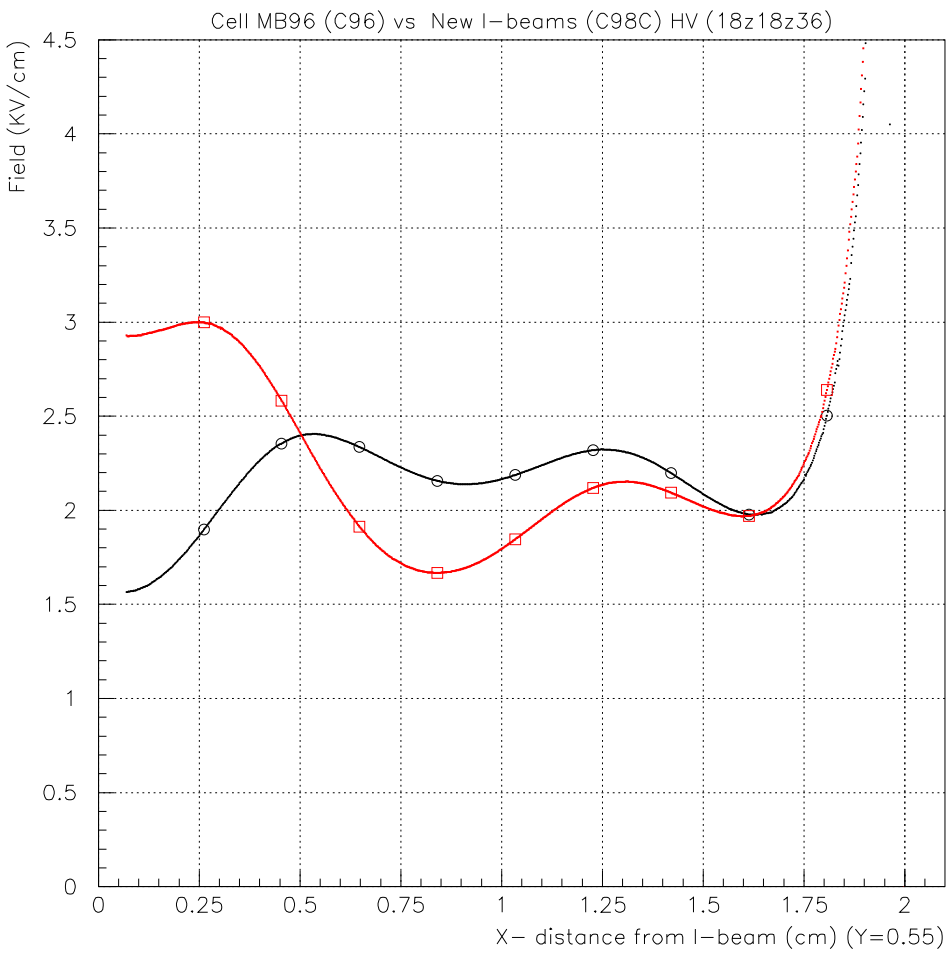

Figure 4: Drift field for MB96 (open circles) and for the cell with new cathodes (open squares)

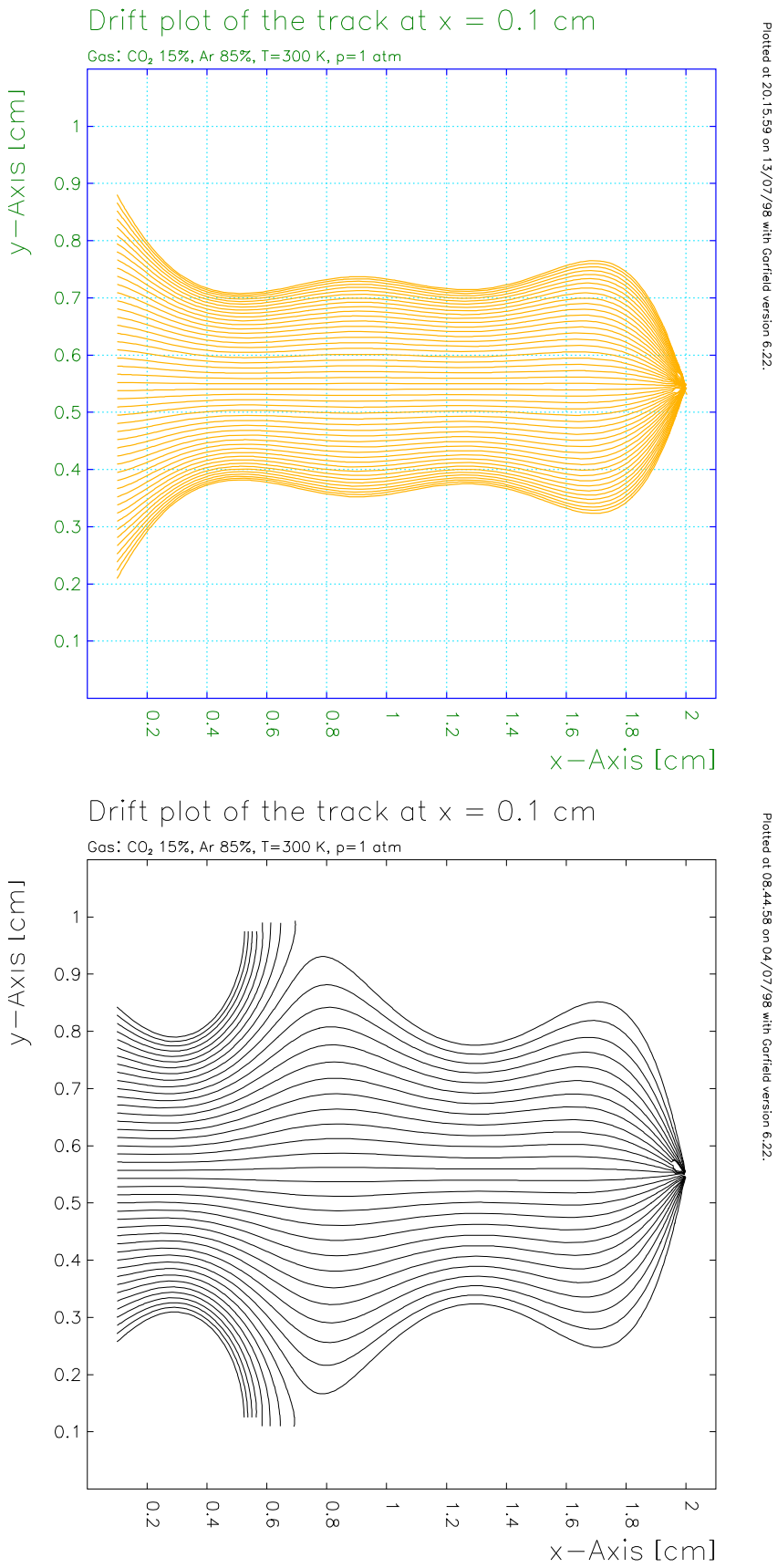

Figure 5: Drift lines from x=0.1cm for MB96 (top) and the cell with new cathodes (bottom)

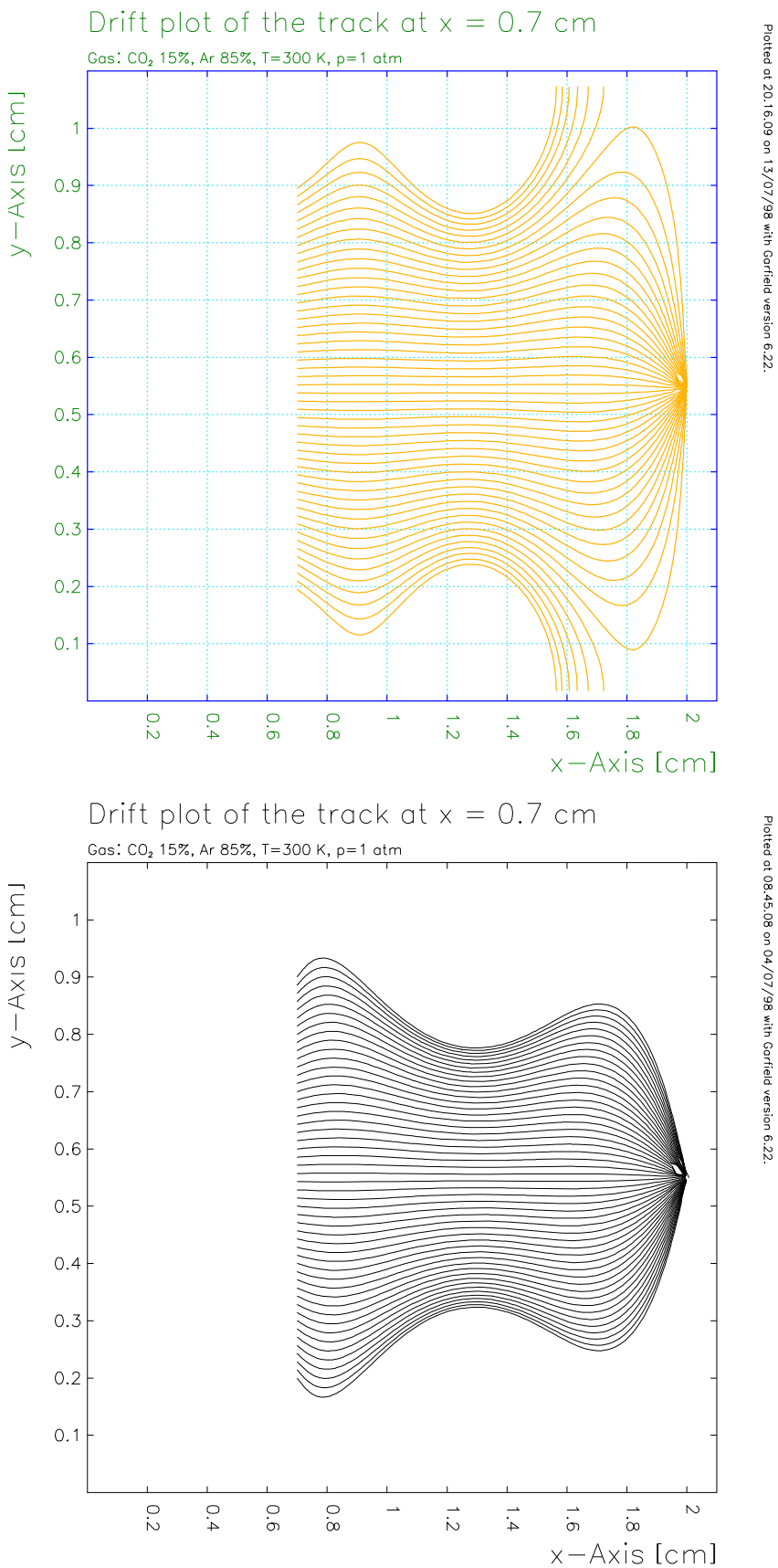

Figure 6: Drift lines from x=0.7cm for MB96 (top) and the cell with new cathodes (bottom)

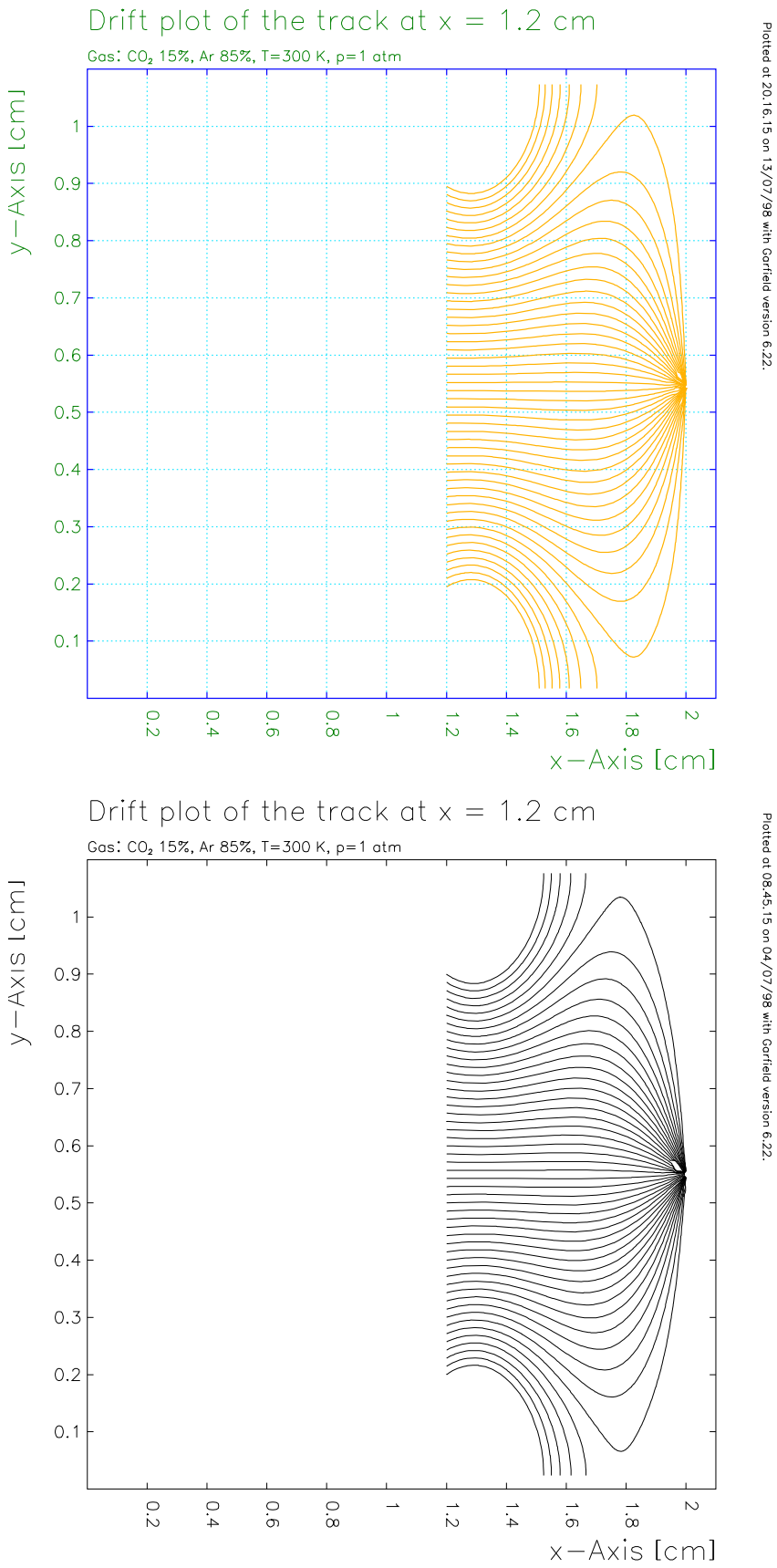

Figure 7: Drift lines from x=1.2cm for MB96 (top) and the cell with new cathodes (bottom)

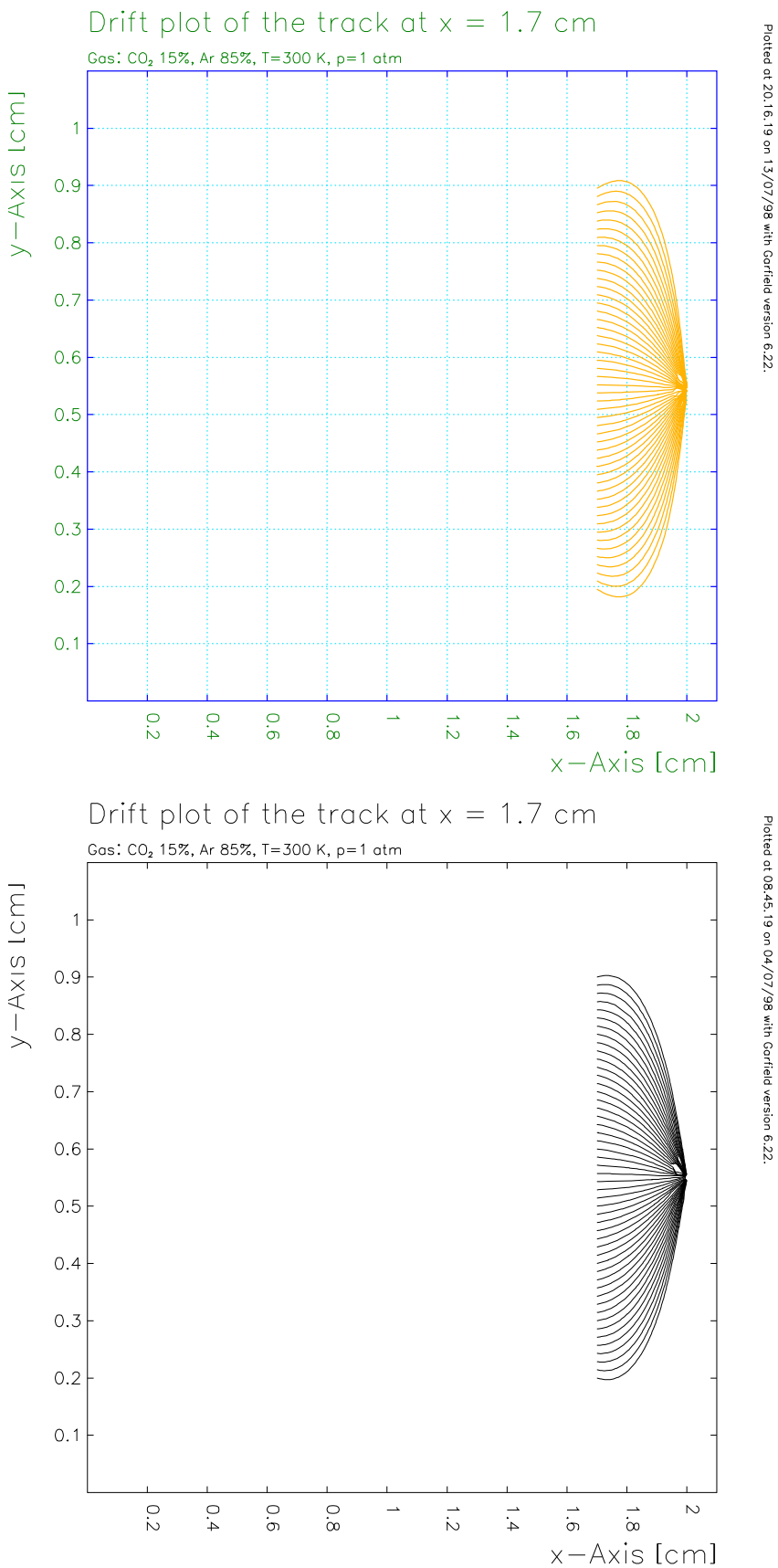

Figure 8: Drift lines from x=1.7cm for MB96 (top) and the cell with new cathodes (bottom)

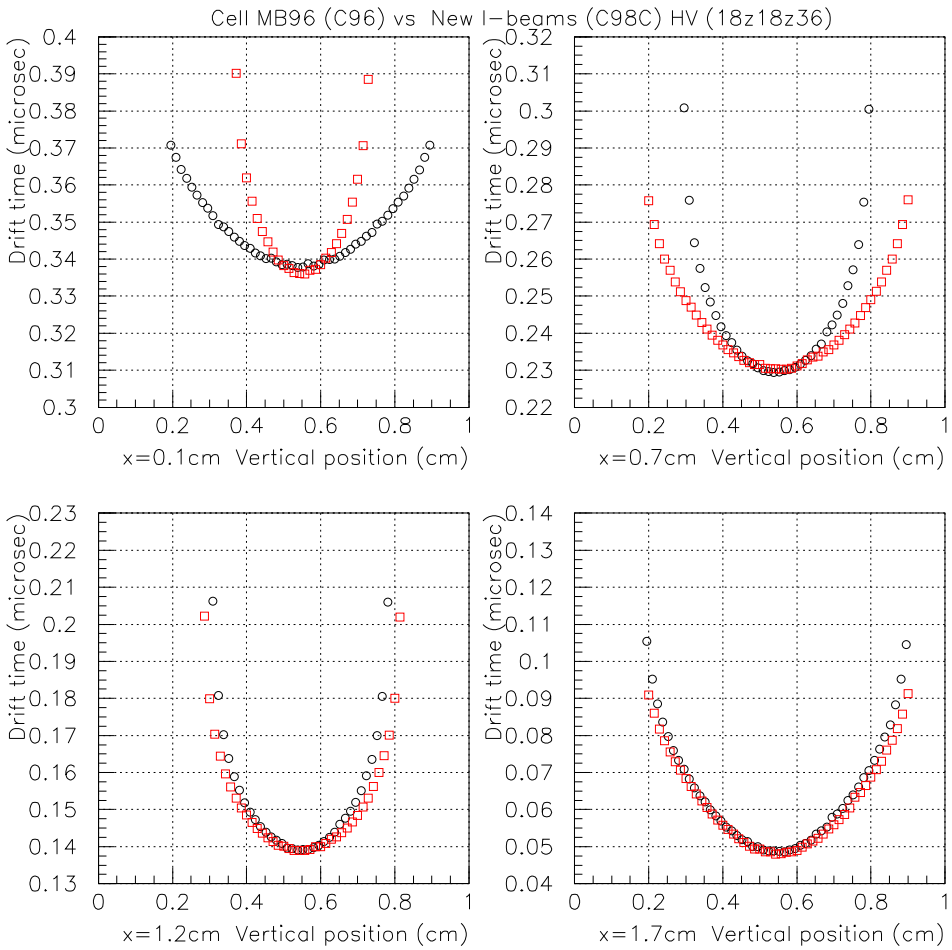

Figure 9: Drift times from different x positions for MB96 (open circles) and for the cell with new cathodes (open squares)

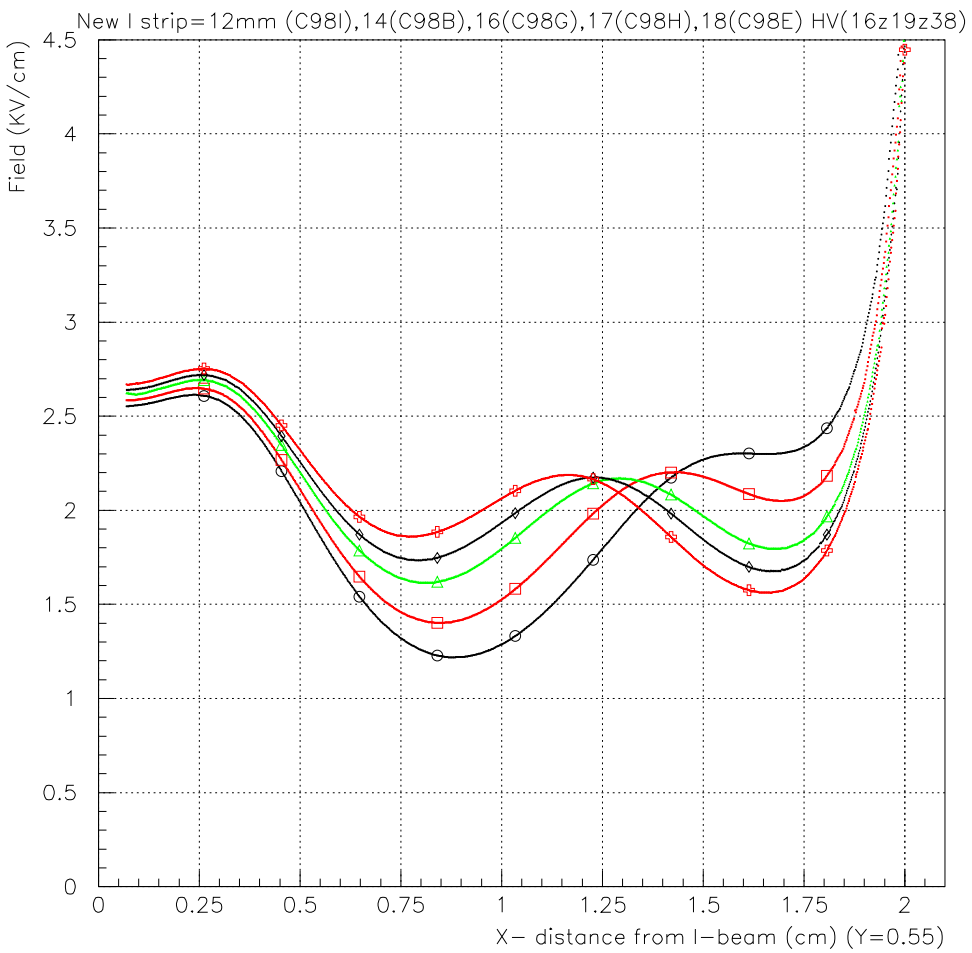

Figure 10: Electric field for the cell with new cathodes and different strip sizes (open circles = 12mm)

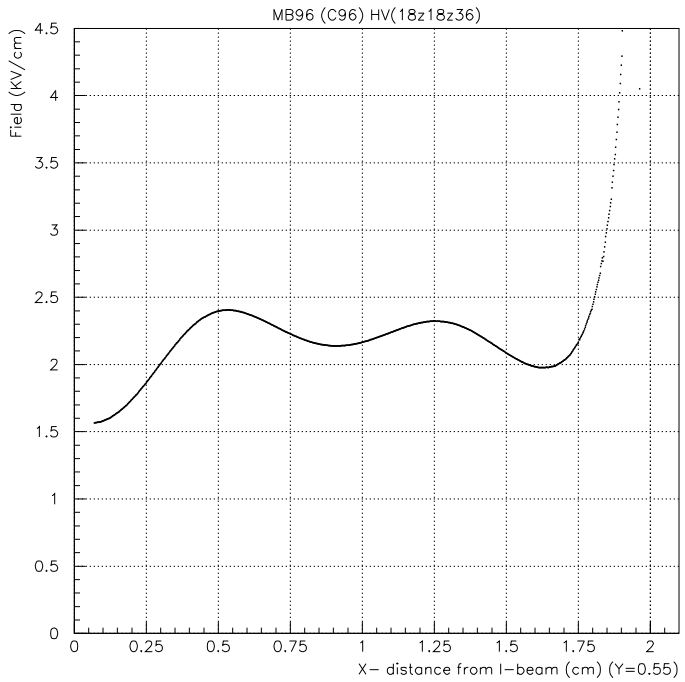

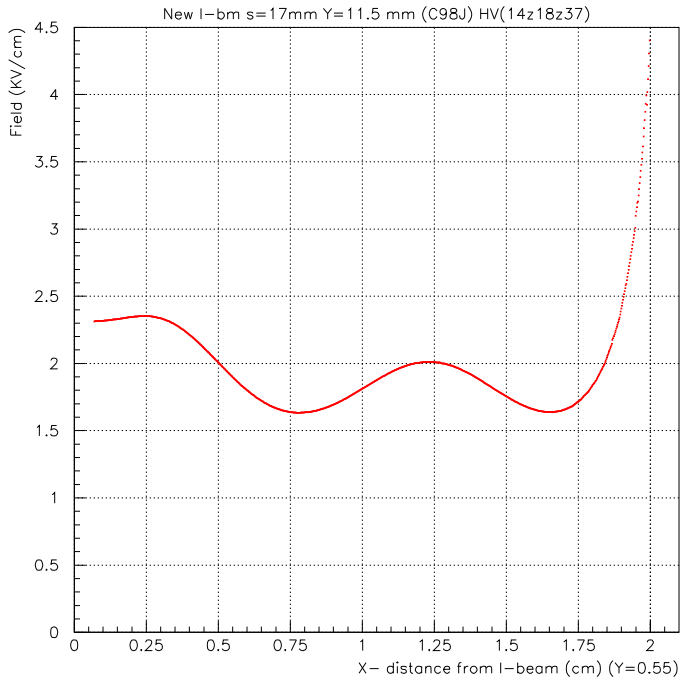

Figure 11: Electric field for MB96 HV(-1800;1800;3600) (top) and for the final cell with HV(-1400;1800;3700) (bottom)

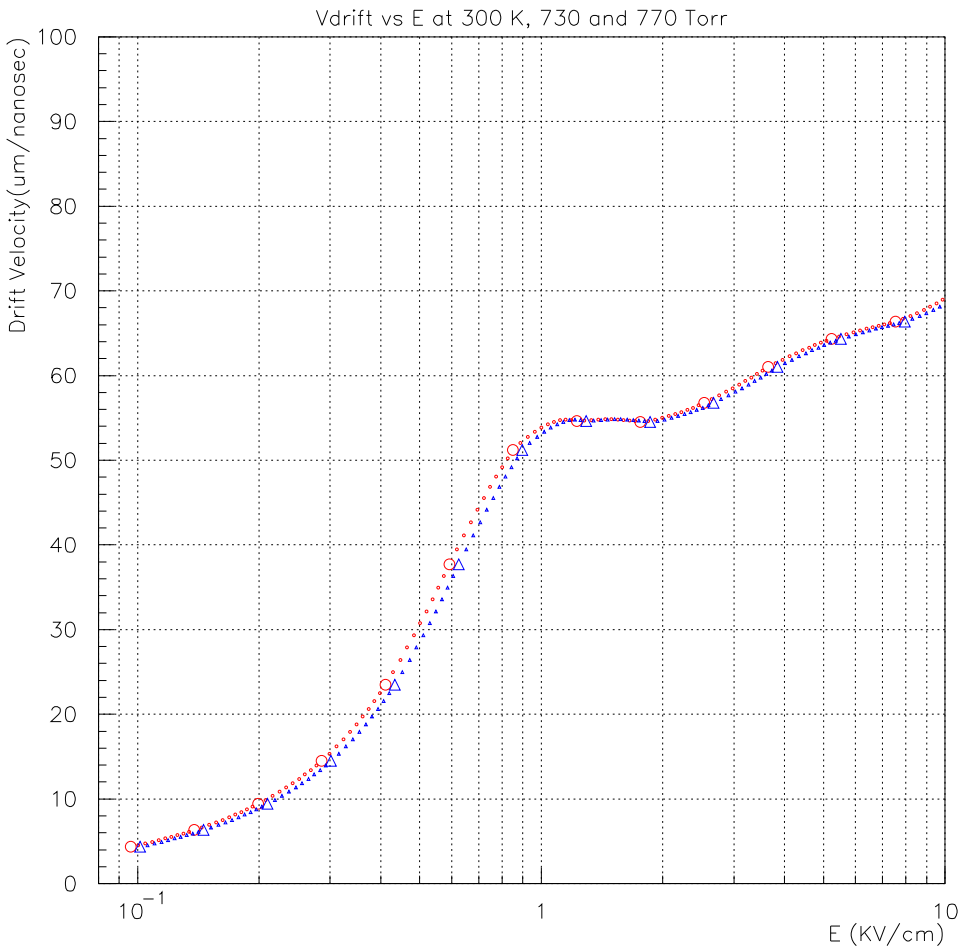

Figure 12: Drift velocity versus Drift field at 730 Torr(open circles) and 770 Torr(open triangles)

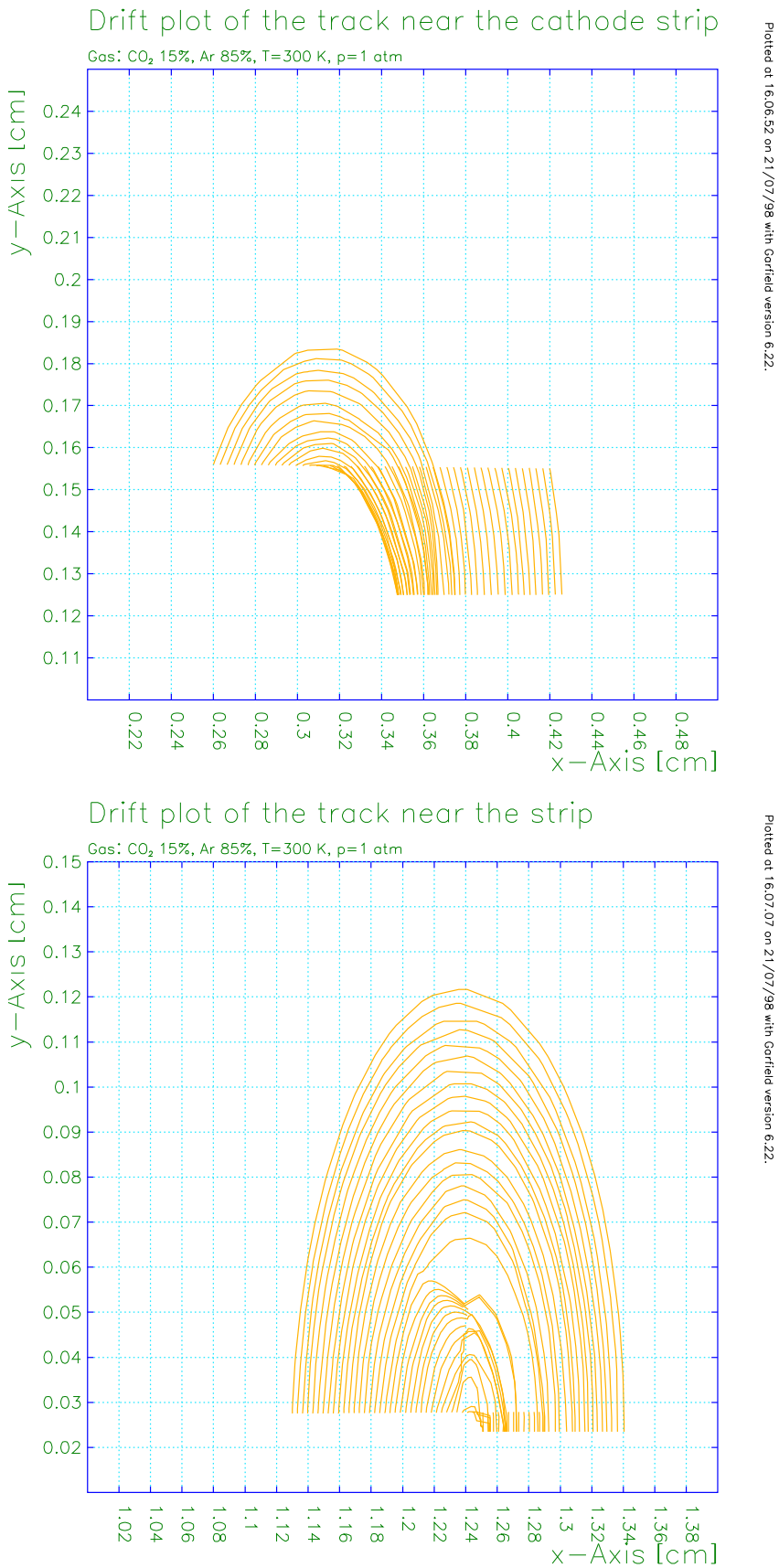

Figure 13: Drift lines of electrons generated near the cathode edge (top) and near the strip edge (bottom)

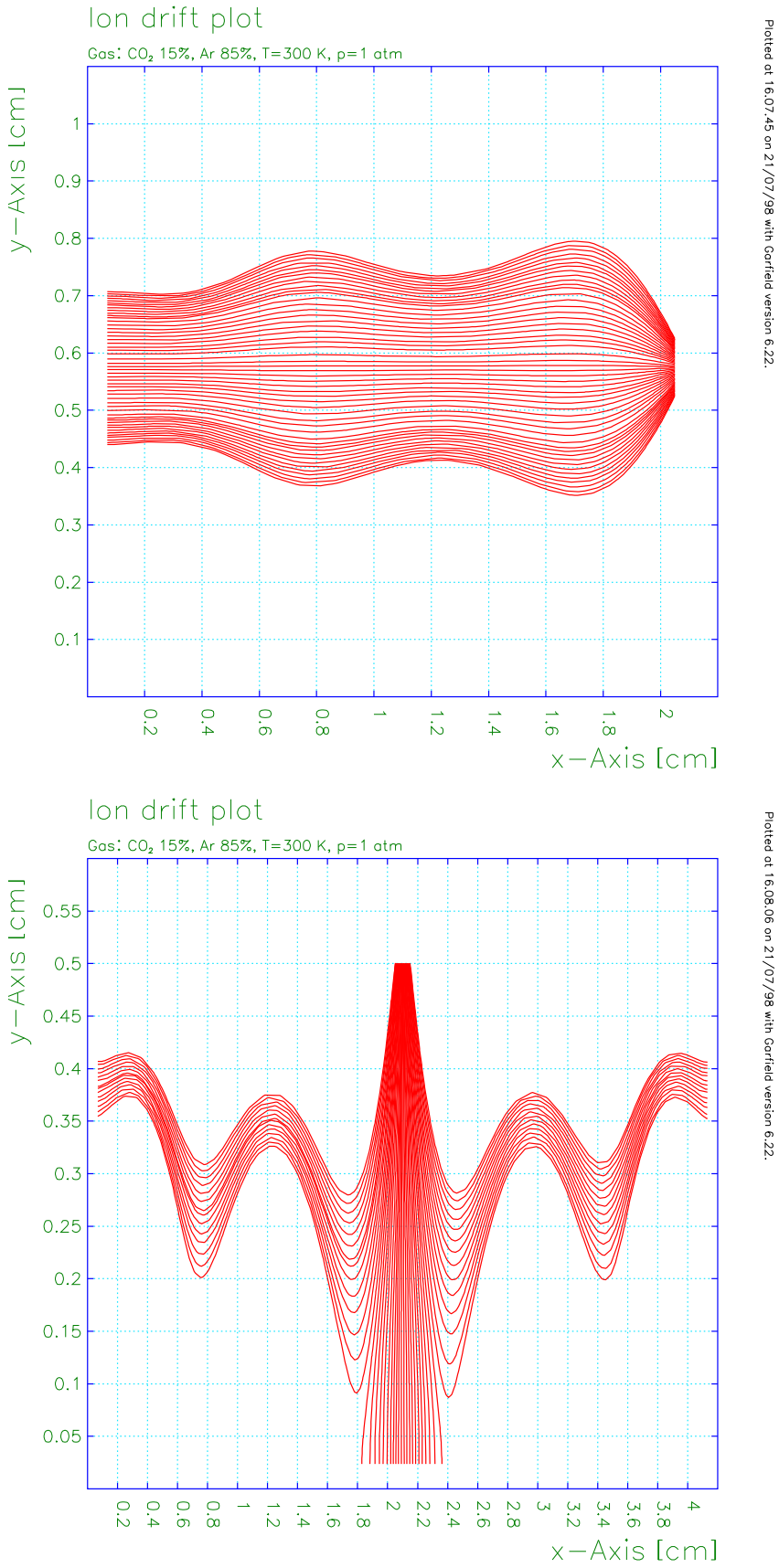

Figure 14: Drift lines of ions generated along y (top) and along x (bottom)